Letter

Temporal disorder in spatiotemporal order

Hongzheng Zhao,[1] Johannes Knolle,[2,3,4] and Roderich Moessner[1]

[1]*Max-Planck-Institut für Physik komplexer Systeme, Nöthnitzer Straße 38, D-01187 Dresden, Germany*

[2]*Department of Physics TQM, Technische Universität München, James-Franck-Straße 1, D-85748 Garching, Germany*

[3]*Munich Center for Quantum Science and Technology (MCQST), D-80799 Munich, Germany*

[4]*Blackett Laboratory, Imperial College London, London SW7 2AZ, United Kingdom*

(Received 6 December 2022; revised 28 August 2023; accepted 29 August 2023; published 15 September 2023)

Time-dependent driving holds the promise of realizing dynamical phenomena absent in static systems. Here, we introduce a correlated random driving protocol to realize a spatiotemporal order that cannot be achieved even by periodic driving, thereby extending the discussion of time translation symmetry breaking to randomly driven systems. We find a combination of temporally disordered micromotion with prethermal stroboscopic spatiotemporal long-range order. This spatiotemporal order remains robust against generic perturbations, with an algebraically long prethermal lifetime where the scaling exponent strongly depends on the symmetry of the perturbation, which we account for analytically.

DOI: 10.1103/PhysRevB.108.L100203

Introduction. Extending the concept of equilibrium phases of matter to nonequilibrium settings attracts perennial interest. Prominent examples involve many-body localization, where the spatial disorder enables eigenstate ordering even at high-energy density, a phenomenon that is disallowed in thermal equilibrium [1,2]. Periodically driven Floquet systems enrich the zoo of nonequilibrium phases, where exotic spatiotemporal behavior can be realized, for instance, in discrete time crystals (DTCs) [3–5] or Floquet topological phases [6,7].

Here we ask, are there types of spatiotemporal ordering that are genuinely new to *temporal* disorder, i.e., randomness in the drive, that lie beyond what can be achieved in conventional Floquet protocols? Closed time-dependent systems generally lack energy conservation [8]. Temporal disorder removes even the remaining quasiconservation as in Floquet systems [9,10], opening up further deleterious energy absorption channels, generally believed to quickly heat up the system until all correlations become trivial and independent of the initial state. Therefore, unlike the spatial disorder which underpins eigenstate order [11–14], temporal disorder generally diminishes interesting dynamical phenomena [15–21] and would therefore seem to hold little promise of exhibiting new spatiotemporal types of order.

Nonetheless, a transient but long-lived prethermal regime can exist if the heating rate is sufficiently controlled [22–32]. In the context of aperiodic driving, a low heating rate can specifically be realized in drive protocols such as random multipolar driving (RMD) or hyperuniform driving with a suppressed low-frequency driving spectrum. Here, the correlated temporal disorder may lead to a tunably polynomially suppressed heating rate for fast drives [33].

Prethermalization opens a long time window that can potentially hold a rich variety of nonequilibrium phases enabled by random drivings. Some cousins of Floquet phases, such as DTCs and anomalous RMD insulators, have been recently discovered in randomly driven systems [19,33–36]. However, none of them answer our question as the temporal disorder in these systems plays the role of an unwanted perturbation, which destabilizes their corresponding Floquet phases, albeit controllably gently. The challenge in moving beyond the Floquet paradigm is thus to employ temporal disorder sufficiently strong to qualitatively modify the dynamical properties while sufficiently weak to keep heating under control.

In this Letter we provide an affirmative answer by presenting a prethermal phase characterized by two types of temporal correlations: Conventional stroboscopic spatiotemporal DTC order coexists with temporally disordered micromotion. This lies outside the established Floquet lore, where micromotions are restricted to follow the stroboscopic time evolution via a deterministic gauge transformation [37]. We evade this constraint by randomly applying a spin-flip operation, leading to a nontrivial π-shifted Fourier spectrum of micromotion that is distinct from that of the driving protocol. The stability of this spatiotemporal order can be analyzed via a Magnus expansion, and we derive a static effective Hamiltonian in the prethermal regime with a suppressed heating rate.

In the following, we first introduce our temporally random driving protocol and elaborate on the prethermal time translation symmetry (TTS) breaking in a soluble instance. We then analytically investigate and numerically verify its stability away from solubility. Upon perturbing from solubility, the prethermal timescale grows algebraically with driving frequency. Remarkably, the scaling exponent strongly depends on the symmetry of the perturbations. Finally, we show that

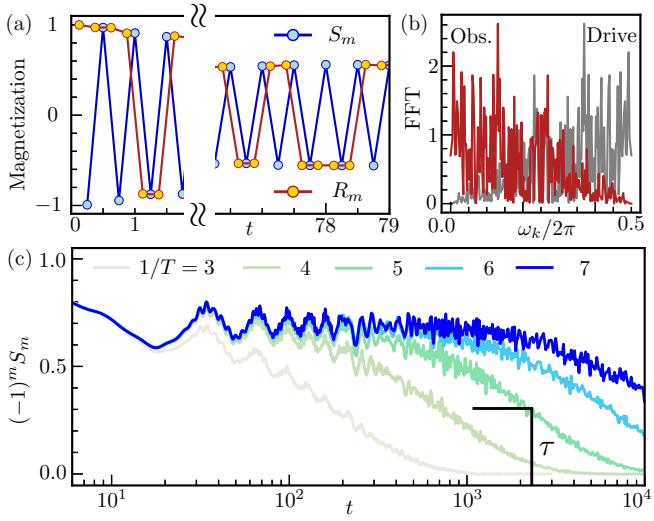

FIG. 1. (a) Distinct temporal correlations emerge for micromotions and stroboscopic times (for system size $L = 26$). (b) Fourier modes of micromotions exhibit a π-shifted spectrum different from the drive, defining another type of TTS breaking. (c) This persists for a long timescale τ, which grows with driving frequency $1/T$. We use $J_z = 1$, $J_x = 0.1$, $J_y = 0.2$, $B_z = 0$, $\delta_r = 0.15$, $L = 18$.

the prethermal phase persists for generic initial states in a localized model. Beyond the example of RMD driving, we generalize our findings for random hyperuniform drivings.

Driving protocol and soluble model. We consider a stepwise drive with two elementary time evolution operators for a spin-1/2 chain of length L,

$$U_0^+ = U_z U_x, \quad U_0^- = U_x U_z,$$
$$U_z = \exp(-iTH_z/2), \quad U_x = \exp(-iTH_x/2), \tag{1}$$

where H_z only involves the nearest-neighbor Ising interaction $H_z = \sum_j J_z \sigma_j^z \sigma_{j+1}^z$ of strength J_z, and a field $H_x = B_x \sum_j \sigma_j^x$ of amplitude B_x. The soluble case is $B_x = \pi/T$, where the operator U_x simplifies to the perfect global spin flip $X = \prod_j \sigma_j^x$ of the Ising Z_2 symmetry. As H_z preserves this Ising symmetry, the product of two U_0^+ operators can be generated by the Hamiltonian H_z as

$$[U_0^+]^2 = \exp(-iTH_z). \tag{2}$$

Consequently, for a Floquet drive generated by U_0^+ and for a Z_2 symmetry broken initial state, the local magnetization at stroboscopic times mT,

$$S_m = \sum_j \langle \sigma_j^z(0)\sigma_j^z(mT)\rangle/L, \tag{3}$$

exhibits period-doubling behavior with respect to the T periodic spin flips [see the blue dots in Fig. 1(a)]. Note, in this soluble case, the oscillation amplitude of S_m never decays. Also, the micromotion is also strictly period doubled, with the magnetization, e.g., at half-integer times $(m + 1/2)T$,

$$R_m = \sum_j \langle \sigma_j^z(0)\sigma_j^z(T/2 + mT)\rangle/L, \tag{4}$$

behaving as that at integer times, as it is connected by the "gauge transformation" U_x.

Now we remove the strict periodicity and randomly apply $U_0^\pm$ according to a random driving sequence $\{y_m\}$ where $y_m = \pm 1$. Its discrete Fourier spectrum, $Y(\omega_k) = \sum_{m=0}^{M-1} y_m \exp(-i\omega_k m)/\sqrt{M}$ where M denotes the length of $\{y_m\}$, exhibits a random distribution in frequency ω_k space with a flat envelope. A similar period-doubling phenomenon still occurs at stroboscopic times as the relation in Eq. (2) equally applies to any product of two operators $U_0^\pm$.

However, the Floquet theorem does not apply and at half-integer times, the magnetization is temporally disordered with the expression $R_m = (-1)^m y_m$: Its value depends on y_m as $U_0^\pm$ determines whether spin flip happens in the first or the second half of a period T; the phase $(-1)^m$ appears as the spin flip changes the sign of magnetization and it disappears after an even number of spin flips. The phase indeed implies a π-shifted spectrum $\widetilde{Y}(\omega_k) = Y(\omega_k + \pi)$ [see proof in the Supplemental Material (SM) [38]], but both of them follow the trivial and structureless frequency spectrum.

However, more interestingly, if $Y(\omega_k)$ is structured, this π shift generally leads to a different spectrum of local observables, hence generalizing the notion of prethermal TTS breaking to random driving protocols. We illustrate this idea by using the family of correlated random drives, the n-RMD protocol with a non-negative integer n which quantifies the temporal correlation [33]. 0-RMD corresponds to the purely random case discussed above. Time evolution is generated by randomly applying one of the multipolar operators $U_n^\pm$, recursively defined as $U_n^\pm = U_{n-1}^\mp U_{n-1}^\pm$. For $n = 1$, the envelope of the Fourier spectrum of the drive reads $Y_1(\omega_k) \sim \sqrt{1 - \cos\omega_k}$ with a linear suppression at $\omega_k = 0$, as shown by gray lines in Fig. 1(b). The π shift for the micromotion persists and results in $\widetilde{Y}_1(\omega_k) \sim \sqrt{1 + \cos\omega_k}$ where the suppression can be clearly observed at $\omega_k = \pi$ (red lines) in Fig. 1(b). Indeed, this behavior exists for the full family of n-RMDs, where the envelope of the Fourier spectrum follows $Y_n(\omega_k) \sim \prod_{j=1}^n \sqrt{1 - \cos(2^{j-1}\omega_k)}$, and a π shift leads to

$$\widetilde{Y}_n(\omega_k) \sim \sqrt{1 + \cos\omega_k} \prod_{j=2}^{n} \sqrt{1 - \cos(2^{j-1}\omega_k)}, \tag{5}$$

for $n \geqslant 2$ (see details in SM [38]). Similar π shifts should also occur for other random protocols as long as the driving sequence has a nontrivial frequency spectrum. As a special feature of the n-RMD protocol, $\widetilde{Y}_n(\omega_k)$ is also a reflection of $Y_n(\omega_k)$ [see Fig. 1(b)], which, however, is not a general property of TTS breaking in randomly driven systems.

Stability. A natural question is whether this TTS breaking persists away from the soluble case. The question of stability is also important for experimental realizations. Naively, the answer would seem to be negative, simply because the continuous Fourier spectrum opens energy absorption channels to destabilize the whole phenomenon.

However, we have previously shown that generic many-body systems driven with an n-RMD protocol can exhibit algebraically long prethermal lifetimes in the high-frequency regime, i.e., the driving frequency is the dominant energy scale of the system [33,39]. By contrast, this is not the case here, as the spin-flip operator U_x acts instantaneously regardless of driving frequency (or, alternatively, requires the field

strength to scale up with driving frequency as $B_x = \pi/T$), and the high-frequency condition is *a priori not* satisfied. Also, the fact the spin-flip operator occurs randomly in time prevents the existence of a deterministic rotating frame where the strong field always vanishes.

We can nonetheless demonstrate that the period-doubling signal persists for a finite but algebraically long lifetime even away from the fine-tuned point. We also find that the lifetime of the prethermal regime strongly depends on the symmetry of the perturbation. To do so, we consider two types of generic perturbations: (i) the imperfection in spin-flip operations with a field strength $B_x = \pi/T + \delta_r$ with δ_r always nonzero in the following discussion; and (ii) perturbations to the Hamiltonian H_z, which (a) either preserve the Z_2 symmetry, satisfying $X\Delta_{Z_2}X = \Delta_{Z_2}$ or (b) violate the symmetry $X\Delta X = -\Delta$. We can show that the concomitant prethermal lifetime scales as (a) $T^{-(2n+3)}$ and (b) $T^{-(2n-1)}$, respectively.

The multipolar operators $U_n^{\pm}$ being unitary, they can be written in the form $U_n^{\pm} = \exp[-i(2^{n-1}T)H_n^{\pm}]$ where $H_n^{\pm}$ is some static Hamiltonian operator. Such a Hamiltonian is generally nonlocal and hard to determine for many-body systems. However, by using a Magnus expansion, $H_n^{\pm} = \sum_{m=0}^{\infty}(2^{n-1}T)^m\Omega_{n,m}^{\pm}$, we can derive its high-frequency expansion that governs the prethermal dynamics [39]. Subsequently we employ a Fermi's golden rule (FGR) argument to predict the scaling of the prethermal lifetime.

We start from the Z_2 preserving perturbations by changing H_z in Eq. (1) to $H = H_z + \Delta_{Z_2}$. It leads to two dipolar operators,

$$U_1^- = e^{-iTH/2}e^{-iT\delta_r\sum_i\sigma_i^x}e^{-iTH/2},$$
$$U_1^+ = e^{-i\frac{T}{2}\delta_r\sum_i\sigma_i^x}e^{-iTH}e^{-i\frac{T}{2}\delta_r\sum_i\sigma_i^x}, \tag{6}$$

where we use the Z_2 symmetry of the perturbed Hamiltonian H and also the property $X^2 = 1$. Consequently, the strong field B_x cancels out and the high-frequency regime is now well defined if $1/T$ is much larger than any other local energy scale. By treating T as a small parameter, for $n = 1$, the Magnus expansion leads to

$$H_1^{\pm} = H_z + \Delta_{Z_2} + \delta_r\sum_i\sigma_i^x + O^{\pm}(T^2), \tag{7}$$

where the zeroth- and the first-order expression is the same for both $U_1^{\pm}$, with differing higher-order terms $O^{\pm}(T^2)$ suppressed for high-frequency drives. Indeed, one can generalize this result (see SM [38]) to larger n, and by induction show that the Hamiltonian, $H_n^{\text{eff}} := \sum_{m=0}^{n}(2^{n-1}T)^m\Omega_{n,m}^{\pm}$, truncated at nth order is the same for $U_n^{\pm}$.

Therefore, the operator H_n^{eff} plays the role of a static effective Hamiltonian generated by an arbitrary sequence of $U_n^{\pm}$. For a generic nonintegrable H_n^{eff}, the system will first locally equilibrate to a prethermal state that can be locally captured by a Gibbs ensemble $\rho_{\text{eff}} \sim \exp(-\beta_{\text{eff}}H_n^{\text{eff}})$. The effective inverse temperature β_{eff} can be determined by the initial expectation value of H_n^{eff}. Additional higher-order terms are generally different for $U_n^{\pm}$ and the most dominant ones' amplitude is $O(T^{n+1})$. They appear randomly in time and induce a heating rate $\gamma \sim T \times [O(T^{n+1})]^2 \sim O(T^{2n+3})$ according to FGR [39]. Hence, the lifetime of the prethermal plateau should scale as $\tau \sim T^{-(2n+3)}$ which we numerically verify below.

Now we discuss the situation with Z_2 symmetry breaking perturbations with $H = H_z + \Delta$. For $n = 1$, the same expression for U_1^- is obtained as in Eq. (6). However, U_1^+ is different,

$$U_1^+ = e^{-i\frac{T}{2}\delta_r\sum_i\sigma_i^x}e^{-iT(H_z-\Delta)}e^{-i\frac{T}{2}\delta_r\sum_i\sigma_i^x}. \tag{8}$$

A similar perturbation expansion leads to

$$H_1^{\pm} = H_z \mp \Delta + \delta_r\sum_i\sigma_i^x + O^{\pm}(T^2). \tag{9}$$

Note the zeroth-order terms differ by the symmetry breaking perturbation Δ. Hence, for $n = 1$ we do not have a well-defined time-independent Hamiltonian to approximate 1-RMD dynamics when the Z_2 symmetry of H is explicitly broken. The existence of a prethermal regime is thus not guaranteed even for large driving frequencies $1/T \to \infty$.

Prethermal behavior can, however, be obtained by increasing the multipolar order. For $n \geqslant 2$, the perturbative expansion H_n^{eff} truncated at the $(n-2)$th order coincides for $U_n^{\pm}$. Consequently, it is the next, $(n-1)$st, order with amplitude $O(T^{n-1})$ which destabilizes the system. The resulting prethermal lifetime scales as $\tau \sim T^{-(2n-1)}$. This scaling equally applies to $n = 1$ if the symmetry breaking Δ is sufficiently weak, i.e., Δ does not strongly couple the initial low-energy state and excited states of H_z. In the following, we support our analysis with numerical simulation via exact diagonalization.

Numerical simulation. We first consider an ordered initial state polarized in the positive z direction, before extending the discussion to more general initial states. We consider a generic nonintegrable Hamiltonian

$$H = H_z + \sum_j J_x\sigma_j^x\sigma_{j+1}^x + J_y\sigma_j^y\sigma_{j+1}^y + B_z\sigma_j^z, \tag{10}$$

to generate U_z. Periodic boundary conditions are used such that the translation invariance permits us to simulate the dynamics for larger system sizes. The spin flip has the fixed rotation imperfection $\delta_r = 0.15$. Nonzero $J_{x,y}$ introduces Z_2 preserving perturbations whereas B_z violate the symmetry.

We first consider a single temporal disorder realization for 1-RMD with symmetry preserving perturbations ($B_z = 0$). In Fig. 1, we plot the magnetization S_m at stroboscopic times as blue dots in Fig. 1(a). Similarly to conventional discrete time crystals, S_m oscillates with a period $2T$ with an amplitude decaying at short times but equilibrating at a nonzero value in the prethermal regime. The magnetization R_m for the micromotions (red) has approximately the same amplitude as S_m but oscillates in a random fashion. The discrete Fourier spectrum of $R_m/|R_m|$ up to the time $t = 100$ is plotted in Fig. 1(b). A clear suppression occurs at $\omega_k = \pi$ as predicted whereas the drive (gray) has a suppression at $\omega_k = 0$, suggesting that the different type of TTS breaking survives perturbations in the prethermal regime. In Fig. 1(c), after averaging over 200 temporally disordered realizations, $(-1)^m S_m$ is plotted and different colors correspond to different driving frequencies. After a short transient period, it relaxes to a nonzero value. The system heats up to infinite temperature after a long timescale, which increases for larger driving frequencies. A similar phenomenon also occurs when Z_2 symmetry is

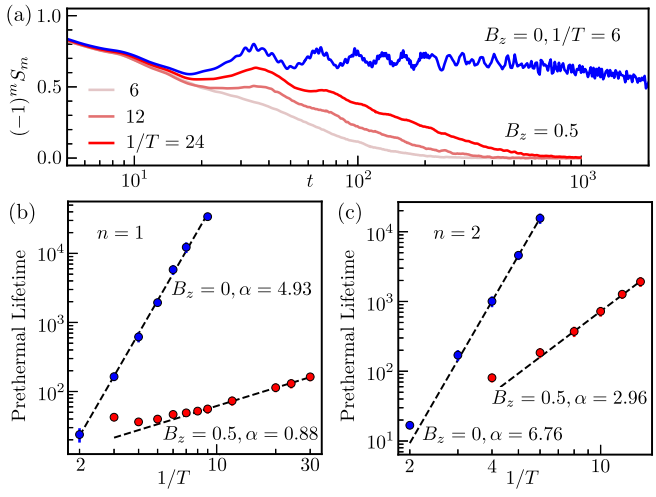

FIG. 2. Prethermal lifetime τ strongly depends on the presence/absence (blue/red lines) of Z_2 symmetry in the perturbation. (a) Dynamics of the stroboscopic magnetization. (b) Algebraic lifetime scaling vs driving frequency $1/T$ for multipolar order $n = 1$. Scaling exponent is approximately $2n + 3$ for Z_2 preserving perturbation with $B_z = 0$, and $2n - 1$ for $B_z = 0.5$ for $n = 1$. (c) Scaling results for $n = 2$. We use $J_z = 1$, $J_x = 0.1$, $J_y = 0.2$, $B_z = 0$, $\delta_r = 0.15$, $L = 18$.

broken ($B_z \neq 0$) as shown in Fig. 2(a). But for a fixed frequency, e.g., $1/T = 6$ (light red), $(-1)^m S_m$ decays much faster than the Z_2 preserving case (blue), highlighting the importance of symmetry in stabilizing the nonequilibrium phases with random drives.

The dependence of the prethermal lifetime can be further quantified by setting a threshold value s_0 for the magnetization. We extract the time t_{s_0} where $(-1)^m S_m$ first drops below s_0, and the prethermal lifetime τ is determined as the average $\langle t_{s_0} \rangle_{s_0}$ for five different threshold values 0.32, 0.32 ± 0.05, 0.32 ± 0.025. The average is performed to reduce numerical noise and the following results do not rely on specific threshold values. In Fig. 2(b), τ is plotted with the error bar denoting the standard deviation and both axes use a log scale. A linear dependence is observed for both types of perturbations, suggesting an algebraic scaling $\tau \sim (1/T)^\alpha$. The exponent α is obtained by a linear fit in the high-frequency regime, and we obtain the scaling exponent $\alpha \approx 2n + 3$ for $B_z = 0$ and $\alpha \approx 2n - 1$ for $B_z \neq 0$. This scaling exponent is tunable by increasing the multipolar order as we verify for $n = 2$ in Fig. 2(c).

The persistence of the spatiotemporal order relies on the fact that the polarized initial state corresponds to a sufficiently low temperature of the effective Hamiltonian H_n^{eff} in the prethermal regime [40]. For more generic initial states at a finite temperature, $(-1)^m S_m$ quickly drops to zero and this prethermal phase will not exist, in accordance with the absence of long-range order at finite temperature in one dimension (1D). This issue can be resolved by introducing, for instance, sufficiently strong spatial disorder to realize the eigenstate order even at high temperatures.

Let us thus consider the Hamiltonian $H = \sum_j (J_z + J_j)\sigma_j^z \sigma_{j+1}^z + J_x \sigma_j^x \sigma_{j+1}^x$, with the spatially disordered couplings

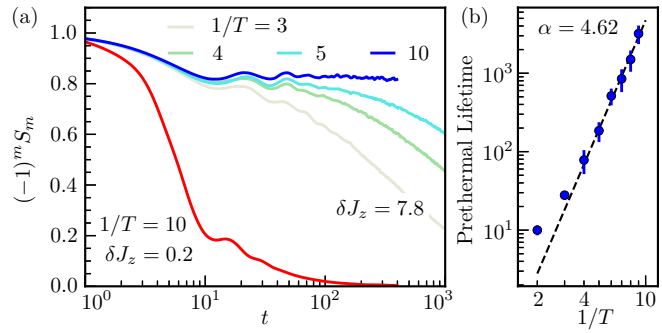

FIG. 3. (a) Dynamics for random product state in the z direction. Prethermal phases persist for sufficiently strong disorder with a lifetime increasing for larger driving frequencies. For weak disorder (red), the spatiotemporal order quickly vanishes. (b) Algebraic lifetime scaling vs frequency with exponent close to $2n + 3$. We use $J_z = 1$, $J_x = 0.1$, $B_z = 0$, $\delta_r = 0.08$, $n = 1$, $L = 16$.

J_j randomly chosen from $[-\delta J_z/2, \delta J_z/2]$. The system starts from a product state containing spins polarized randomly in the $\pm z$ direction with total magnetization zero. We perform 400 simulations to average over different initial states, and spatial and temporal disorder realizations with the multipolar order $n = 1$. The magnetization $(-1)^m S_m$ is plotted in Fig. 3(a). For sufficiently strong disorder $\delta J_z = 7.8$ (blue), with localization established, the system maintains strong memory of the initial state, $(-1)^m S_m \approx 0.8$, in the prethermal regime. We extract the prethermal lifetime when the magnetization starts deviating from the prethermal plateau by using five different threshold values 0.76, 0.76 ± 0.02, 0.76 ± 0.01, and plot it in Fig. 3(b) where an algebraic scaling is observed. We do not observe notable finite-size effects in our simulation (see details in SM [38]). The fitted scaling exponent is close to $2n + 3$ as predicted. In contrast, for a weak disorder $\delta J_z = 0.2$ (red), eigenstates of the truncated effective Hamiltonian are not ordered at a high-energy density, hence, the system quickly heats up with a vanishing magnetization.

Discussion. We show that a different type of spatiotemporal order absent in Floquet systems can be achieved by structured random protocols, which is manifest through a π-shifted spectrum of the dynamics of local observables compared to the spectrum of the drive. Many-body localization is employed here to stabilize the Z_2 ordering in the prethermal regime. It can be alternatively achieved by using higher dimensional spin models or long-range interactions in 1D [40–43], and classical spin models will also be suitable for large-scale numerical simulations [44,45].

We emphasize that, although our results build on the concrete n-RMD protocol, this alternate type of TTS breaking is quite generic. To provide another concrete example, consider a driving protocol with the Hamiltonian $H = H_z + \sum_j J_x \sigma_j^x \sigma_{j+1}^x$ to generate the time evolution and apply $U_x = \exp[-i(1 + \delta_r')\pi/2 \sum_j \sigma_j^x]$ with imperfection δ_r' to flip the spins instantaneously at time $t = mT + T/2 + \delta t_m$ for integer m and random $\delta t_m \in [\delta t_{\max}, \delta t_{\max}]$. This randomness can be chosen to be "hyperuniform," i.e., with suppressed large-scale fluctuations [46,47], leading to an algebraic suppression of low frequencies similar to the RMD sequence but with a

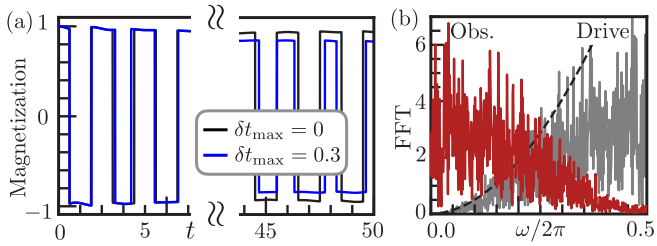

FIG. 4. (a) Dynamics of the magnetization. For the blue line, spins flip randomly according to a hyperuniform sequence, while for the black line, spins flip deterministically. System size $L = 20$ and rotation imperfection $\delta_r' = 0.01$. (b) Fourier modes of magnetization exhibit a π-shifted spectrum different from the drive. The algebraic suppression (dashed black) has an exponent $\alpha/2$. We use $J_z = 1, J_x = 0.2, \alpha = 3.8, L = 16, \delta_r' = 0, \delta t_{\max} = 0.1, T = 1$ for the numerical simulation.

continuously tunable scaling exponent $\alpha/2$ (see details in the SM [38]). In Fig. 4(a), starting from the initial state $\prod_i |\uparrow\rangle$, we plot the time evolution of the magnetization $\sum_j \langle \sigma_j^z \rangle / L$ where the regular period-doubling behavior occurs stroboscopically. In contrast, the random micromotions exhibit the π-shifted spectrum as shown in Fig. 4(b). Such a pattern can also be long lived by choosing a small $\delta t_{\max}$ (see SM [38]). A systematic investigation of the prethermal lifetime and its relation to hyperuniformity is an intriguing subject for future study.

Another important feature is the symmetry dependence of the prethermal lifetime scaling. An intriguing direction for the future is then a systematic symmetry classification of heating dynamics. Similar questions are also worth studying in Floquet systems and quasiperiodically driven systems [17,36,48–50].

Going forward, we anticipate the extension of our protocol to Floquet topological phases and their generalizations [51,52]. In Ref. [7], the soluble limit involves four-step hopping processes and a fifth-step random disorder potential. One can reshuffle the fifth step, such that particle hopping is temporally disordered while stroboscopic dynamics remain deterministic. Investigating the prethermal phenomenon away from this soluble limit will be worth pursuing in the future.

Acknowledgments. This work is in part supported by the Deutsche Forschungsgemeinschaft under cluster of excellence ct.qmat (EXC 2147, Project-ID 390858490). The research is part of the Munich Quantum Valley, which is supported by the Bavarian state government with funds from the Hightech Agenda Bayern Plus.

[1] R. Nandkishore and D. A. Huse, Annu. Rev. Condens. Matter Phys. **6**, 15 (2015).
[2] D. A. Abanin, E. Altman, I. Bloch, and M. Serbyn, Rev. Mod. Phys. **91**, 021001 (2019).
[3] V. Khemani, A. Lazarides, R. Moessner, and S. L. Sondhi, Phys. Rev. Lett. **116**, 250401 (2016).
[4] D. V. Else, B. Bauer, and C. Nayak, Phys. Rev. Lett. **117**, 090402 (2016).
[5] N. Y. Yao, A. C. Potter, I.-D. Potirniche, and A. Vishwanath, Phys. Rev. Lett. **118**, 030401 (2017).
[6] T. Kitagawa, E. Berg, M. Rudner, and E. Demler, Phys. Rev. B **82**, 235114 (2010).
[7] P. Titum, E. Berg, M. S. Rudner, G. Refael, and N. H. Lindner, Phys. Rev. X **6**, 021013 (2016).
[8] A. Lazarides, A. Das, and R. Moessner, Phys. Rev. E **90**, 012110 (2014).
[9] D. A. Abanin, W. De Roeck, and F. Huveneers, Phys. Rev. Lett. **115**, 256803 (2015).
[10] T. Kuwahara, T. Mori, and K. Saito, Ann. Phys. **367**, 96 (2016).
[11] D. A. Huse, R. Nandkishore, V. Oganesyan, A. Pal, and S. L. Sondhi, Phys. Rev. B **88**, 014206 (2013).
[12] D. Pekker, G. Refael, E. Altman, E. Demler, and V. Oganesyan, Phys. Rev. X **4**, 011052 (2014).
[13] A. Chandran, V. Khemani, C. R. Laumann, and S. L. Sondhi, Phys. Rev. B **89**, 144201 (2014).
[14] J. Randall, C. Bradley, F. van der Gronden, A. Galicia, M. Abobeih, M. Markham, D. Twitchen, F. Machado, N. Yao, and T. Taminiau, Science **374**, 1474 (2021).
[15] J. Marino and A. Silva, Phys. Rev. B **86**, 060408(R) (2012).
[16] M.-T. Rieder, L. M. Sieberer, M. H. Fischer, and I. C. Fulga, Phys. Rev. Lett. **120**, 216801 (2018).
[17] D. M. Long, P. J. Crowley, and A. Chandran, Phys. Rev. B **105**, 144204 (2022).
[18] G. Guarnieri, M. T. Mitchison, A. Purkayastha, D. Jaksch, B. Buča, and J. Goold, Phys. Rev. A **106**, 022209 (2022).
[19] H. Zhao, M. S. Rudner, R. Moessner, and J. Knolle, Phys. Rev. B **105**, 245119 (2022).
[20] X. Mi, M. Ippoliti, C. Quintana, A. Greene, Z. Chen, J. Gross, F. Arute, K. Arya, J. Atalaya, R. Babbush *et al.*, Nature (London) **601**, 531 (2022).
[21] S. Bhattacharjee, S. Bandyopadhyay, and A. Dutta, Phys. Rev. A **106**, 022206 (2022).
[22] D. V. Else, B. Bauer, and C. Nayak, Phys. Rev. X **7**, 011026 (2017).
[23] S. A. Weidinger and M. Knap, Sci. Rep. **7**, 45382 (2017).
[24] P. T. Dumitrescu, R. Vasseur, and A. C. Potter, Phys. Rev. Lett. **120**, 070602 (2018).
[25] D. V. Else, W. W. Ho, and P. T. Dumitrescu, Phys. Rev. X **10**, 021032 (2020).
[26] D. J. Luitz, R. Moessner, S. L. Sondhi, and V. Khemani, Phys. Rev. X **10**, 021046 (2020).
[27] T. Mori, Phys. Rev. Lett. **128**, 050604 (2022).
[28] K. Viebahn, J. Minguzzi, K. Sandholzer, A.-S. Walter, M. Sajnani, F. Görg, and T. Esslinger, Phys. Rev. X **11**, 011057 (2021).
[29] C. Fleckenstein and M. Bukov, Phys. Rev. B **103**, 144307 (2021).
[30] W. Beatrez, O. Janes, A. Akkiraju, A. Pillai, A. Oddo, P. Reshetikhin, E. Druga, M. McAllister, M. Elo, B. Gilbert *et al.*, Phys. Rev. Lett. **127**, 170603 (2021).

[31] A. Rubio-Abadal, M. Ippoliti, S. Hollerith, D. Wei, J. Rui, S. L. Sondhi, V. Khemani, C. Gross, and I. Bloch, Phys. Rev. X **10**, 021044 (2020).
[32] M. Collura, A. De Luca, D. Rossini, and A. Lerose, Phys. Rev. X **12**, 031037 (2022).
[33] H. Zhao, F. Mintert, R. Moessner, and J. Knolle, Phys. Rev. Lett. **126**, 040601 (2021).
[34] S. Choudhury and W. V. Liu, arXiv:2109.05318.
[35] C. I. Timms, L. M. Sieberer, and M. H. Kolodrubetz, Phys. Rev. Lett. **127**, 270601 (2021).
[36] P. P. Zheng, C. I. Timms, and M. H. Kolodrubetz, arXiv:2206.13926.
[37] M. Bukov, L. D'Alessio, and A. Polkovnikov, Adv. Phys. **64**, 139 (2015).
[38] See Supplemental Material at http://link.aps.org/supplemental/10.1103/PhysRevB.108.L100203 for the definition of the Fourier spectrum of the drive as well as the local observable dynamics. We also illustrate the derivation of the effective Hamiltonian, system size dependence, and more details about the hyperuniform drive.
[39] T. Mori, H. Zhao, F. Mintert, J. Knolle, and R. Moessner, Phys. Rev. Lett. **127**, 050602 (2021).
[40] A. Pizzi, A. Nunnenkamp, and J. Knolle, Phys. Rev. Lett. **127**, 140602 (2021).
[41] F. Machado, D. V. Else, G. D. Kahanamoku-Meyer, C. Nayak, and N. Y. Yao, Phys. Rev. X **10**, 011043 (2020).
[42] A. Kyprianidis, F. Machado, W. Morong, P. Becker, K. S. Collins, D. V. Else, L. Feng, P. W. Hess, C. Nayak, G. Pagano *et al.*, Science **372**, 1192 (2021).
[43] B. Ye, F. Machado, and N. Y. Yao, Phys. Rev. Lett. **127**, 140603 (2021).
[44] O. Howell, P. Weinberg, D. Sels, A. Polkovnikov, and M. Bukov, Phys. Rev. Lett. **122**, 010602 (2019).
[45] M. Yue and Z. Cai, Phys. Rev. B **107**, 094313 (2023).
[46] S. Torquato, Phys. Rep. **745**, 1 (2018).
[47] P. J. D. Crowley, C. R. Laumann, and S. Gopalakrishnan, Phys. Rev. B **100**, 134206 (2019).
[48] A. Verdeny, J. Puig, and F. Mintert, Z. Naturforsch. A **71**, 897 (2016).
[49] F. Nathan, R. Ge, S. Gazit, M. S. Rudner, and M. Kolodrubetz, Phys. Rev. Lett. **127**, 166804 (2021).
[50] A. J. Friedman, B. Ware, R. Vasseur, and A. C. Potter, Phys. Rev. B **105**, 115117 (2022).
[51] M. Wampler, B. J. J. Khor, G. Refael, and I. Klich, Phys. Rev. X **12**, 031031 (2022).
[52] P. T. Dumitrescu, J. G. Bohnet, J. P. Gaebler, A. Hankin, D. Hayes, A. Kumar, B. Neyenhuis, R. Vasseur, and A. C. Potter, Nature (London) **607**, 463 (2022).